Available online at www.sciencedirect.com

ScienceDirect

IFAC Papers Online CONFERENCE PAPER ARCHIVE

IFAC PapersOnLine 54-11 (2021) 43–48

Optimizing grinding mill performance using extremum seeking control

L. Ziolkowski * **J. D. le Roux** *,1 **I. K. Craig** *

* *Department of Electrical, Electronic and Computer Engineering, University of Pretoria, Pretoria, South Africa*

Abstract: A semi-autogenous grinding mill is simulated with an extremum seeking controller to maximize the performance of the mill using grind curves. Grind curves map the essential performance measures of a grinding mill to the manipulable variables. The curves vary with the changes in the feed ore characteristic but show generic parabolic features with extremums. The extremum seeking controller searches along the unknown input-output map using periodic perturbations to steer the process towards an unknown optimum. In this study the controller searches along the grind curves to either optimize the mill throughput or grind by means of the mill feed or rotational speed. The proposed controller will reduce the need for a plant operator to select the optimal operating region. Since the controller is agnostic to the process model, it will also eliminate the tedious process of developing an accurate plant model for model-based control.

Keywords: Extremum seeking, grinding mill, process optimization, mineral processing

1. INTRODUCTION

Comminution is the primary operation within mineral processing plants where the run-of-mine ore material is reduced to fine particles to liberate the valuable minerals within the ore. In run-of-mine mineral processing plants, the feed ore composition is regularly changing and the feed ore characteristics such as hardness and size distribution vary, affecting the throughput and grind quality (Maritz et al., 2019). Manually operating a grinding mill requires frequent monitoring and setpoint adjustments to compensate for these disturbances and maintain the process at suitable operating conditions to maximize the net economic benefit. A significant source of economic loss in process plants is typically attributed to poorly chosen operating conditions, and further losses are due to the deviations from the chosen operating conditions (Hodouin, 2011). Grinding mill circuits are challenging to operate manually and to run at optimal operating conditions due to the complex process behaviour, various unknown process disturbances and strongly-coupled variables (Zhou et al., 2016). In the absence of a high-level supervisory controller, the plant operator is often responsible for choosing suitable operating conditions for the grinding mill. However, insufficient knowledge of the process behaviour in addition to the unknown time-varying factors such as the feed ore variation results in sub-optimal operation of the grinding mill.

Grinding mills are controlled to satisfy operational objectives, which are interrelated due to the inverse relationships that exists between the controlled variables. A trade-off has to be considered between improving the grind quality, maximizing the throughput and decreasing power consumption (Wei and Craig, 2009). Increasing the rate at which the material is processed through the grinding mill can be achieved at the expense of decreased grind quality, but it is crucial that the ore material is sufficiently ground to a specific consistent particle size to achieve effective separation in downstream processes. However, over-grinding produces a product that may be too fine for separation, while reducing the throughput and increasing the energy consumption. Consequently, a poor recovery rate, increased energy consumption or decreased throughput results in diminishing economic gains (le Roux and Craig, 2019).

There is an incentive to employ a real-time supervisory controller that ensures the process is continuously tracking the optimal operating conditions that satisfy the operational objectives. The optimizer would operate in a region nearer to the optimal operating region compared to the periodic setpoint choices of a plant operator as illustrated in Fig. 1. Lu et al. (2020) illustrates how extremum seeking control can be applied to optimize grinding mill perfor-

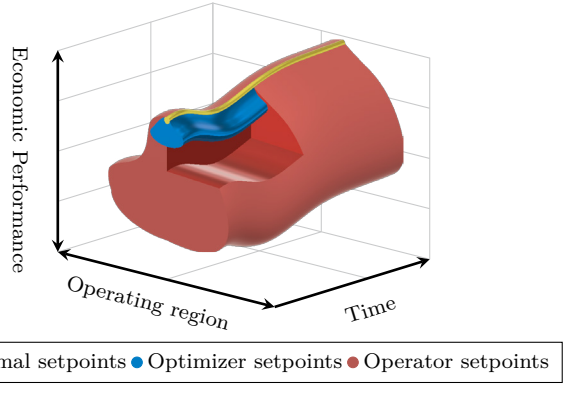

Fig. 1. Economic performance of a grinding mill as a function of the operating conditions.

[1] Corresponding author, E-mail: derik.leroux@up.ac.za

10.1016/j.ifacol.2021.10.048

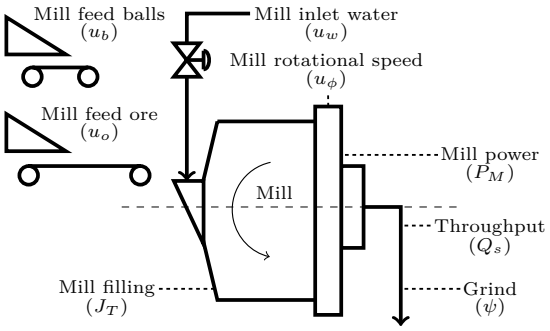

Fig. 2. A semi-autogenous (SAG) mill.

mance, albeit not with the use of grind curves. Grind curves are useful as it maps the performance measures of a grinding mill to the mill load and rotational speed, and indicates where the extremums exist (Powell et al., 2009). The contribution of this paper is to demonstrate the value of grind curves combined with extremum seeking control to maximize the performance of a grinding mill, without requiring detailed knowledge of the process behaviour. The grinding process is described in Section 2, grind curves are discussed in Section 3 and the process model is described in Section 4. The extremum seeking controller is presented in Section 5 and the simulated results are presented in Section 6. Section 7 concludes the paper.

2. PROCESS DESCRIPTION

A SAG mill is illustrated in Fig. 2. The nomenclature is shown in Table 1. The mill receives three streams: mined ore (u_o), water (u_w), and steel balls (u_b). The mill charge is a mixture of grinding media and slurry. Grinding media refers to the steel balls and rocks which break the ore, and slurry refers to the mixture of solids and water. The fraction of the mill filled with charge is denoted by J_T.

The mill is rotated along its longitudinal axis at a fraction of the critical mill speed (u_ϕ) which creates a cascading motion of charge inside the mill. The cascading motion causes the ore to break through impact breakage, abrasion, and attrition. The ground ore in the mill mixes with water to create a slurry which is discharged through an end-discharge grate. Ore too large to pass through the end-discharge grate are referred to as *rocks* and must be broken further. All ore small enough to pass through the end-discharge grate are referred to as *solids*. The flow rate of solids and water discharging from the mill is given by Q_s and Q_w respectively. Q_s is the volumetric throughput of solids through the mill and is equal to u_o/ρ_o at steady-state where ρ_o is the ore density.

Table 1. Description of comminution circuit variables.

Variable	Unit	Description
J_T	(-)	Fraction of mill volume filled with charge
P_M	(kW)	Mill power draw
Q_w	(m^3/h)	Water discharge flow rate
Q_s	(m^3/h)	Solids discharge flow rate
Q_f	(m^3/h)	Fines discharge flow rate
ρ_o	(t/m^3)	Ore density
ψ	(-)	Grind (volume fraction of particles in discharge < 75 μm)
u_b	(t/h)	Feed rate of steel balls
u_o	(t/h)	Feed rate of ore
u_w	(m^3/h)	Flow rate of feed water
u_ϕ	(-)	Fraction of critical mill speed

The aim of the grinding mill is to grind the ore to below a specification size, e.g., 75 μm. The mill grind (ψ) is the volume fraction of material in the discharge of the mill below the specification size. The broken ore below the specification size are referred to as *fines*. Note, whereas solids refer to all ore small enough to discharge from the mill, fines refer to the portion of solids smaller than the specification size. The discharge flow rate of fines from the mill is given by Q_f.

Grinding mills are typically operated to maximize Q_s while keeping the grind particle size within an acceptable range. The net revenue generated from an increased throughput is often perceived to exceed the economic value that could be generated from the losses incurred in the separation process due to the decreased grind quality. However, depending on the market and ore availability it could be beneficial to maintain a set throughput and minimize the product particle size variation to increase recovery rates (Bouffard, 2015; le Roux and Craig, 2019). The mill charge is primarily controlled to achieve the desired throughput by manipulating u_o and u_w. However, in situations where the feed ore hardness or size varies and the mill charge cannot be effectively controlled to compensate for the disturbances, manipulating u_ϕ adds an additional degree of freedom to control Q_s or ψ (Edwards et al., 2002; le Roux et al., 2016).

3. GRIND CURVES

The performance indicators of a grinding mill circuit are defined by the throughput (Q_s), grind (ψ) and power consumption (P_M). Grind curves describe the relationships between these performance indicators as a function of J_T and u_ϕ (van der Westhuizen and Powell, 2006). A notable characteristic of grind curves is that they are parabolic and indicate the peaks of the performance indicators as the mill load is varied for different constant mill speeds, as shown in Figs. 3 and 4. Importantly, as the feed ore characteristics such as hardness vary, the peaks of the performance indicators shift while the parabolic trend is retained for different ore types (Powell et al., 2001).

The peaks of the grind curve data in van der Westhuizen and Powell (2006) are provided in Table 2 and used to produce the 3-D surface map of the performance indicators as a function of J_T and u_ϕ as shown in Figs. 3 and 4. The performance indicators are fit separately as quadratic polynomials as a function of J_T for each mill speed. Multiple linear regression is used to fit the performance indicators as cubic polynomials as a function of u_ϕ. The surface map of the grind curves clearly indicate the trade-off that has to be made when optimizing either Q_s or ψ.

Table 2. Performance indicator peaks from van der Westhuizen and Powell (2006).

Mill speed	Throughput		Grind	
u_ϕ (−)	J_T (−)	Q_s (m^3/h)	J_T (−)	ψ (−)
0.75	0.35	157.0	0.33	0.56
0.70	0.31	120.7	0.37	0.69
0.65	0.23	93.3	0.58	0.94
0.60	0.18	96.7	0.63	1.00

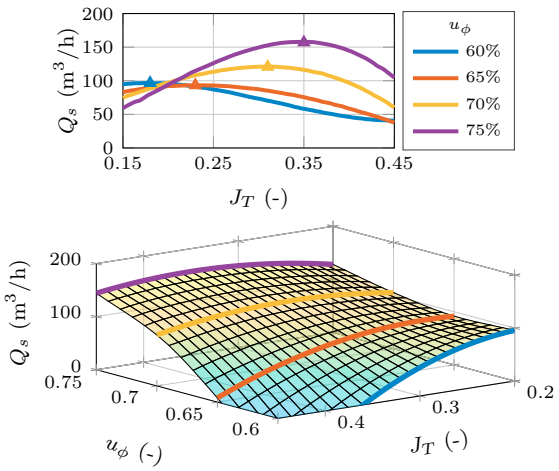

Fig. 3. Grind curves for throughput (Q_s) reproduced from van der Westhuizen and Powell (2006) (top), 3-D surface map of Q_s (bottom).

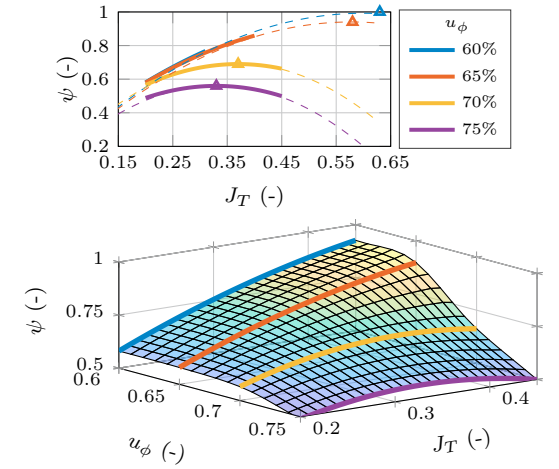

Fig. 4. Grind curves for grind (ψ) reproduced from van der Westhuizen and Powell (2006) (top), 3-D surface map of ψ (bottom).

Assuming that J_T is kept constant, an increase in Q_s can be achieved by increasing u_ϕ at the cost of a decrease in ψ and vice-versa. Alternatively, by maintaining u_ϕ constant, Q_s is maximized by increasing J_T up to an extremum after which Q_s begins to decrease. As the grinding mill begins to overfill, less breakage occurs and oversized ore accumulates in the mill. Maximizing ψ is usually not as beneficial as there is a maximum acceptable grind quality, after which the product is too fine for the separation process to perform optimally (le Roux and Craig, 2019). In addition, over-grinding increases energy consumption, therefore, it is common for the operational objectives of a grinding mill circuit to maximize Q_s until the minimum acceptable ψ is achieved.

4. MODEL DESCRIPTION

A dynamic non-linear model of a grinding mill (le Roux et al., 2013) is fit using the step-wise procedure as described in le Roux et al. (2020) using the grind curve data from van der Westhuizen and Powell (2006). The model produces a realistic dynamic and steady-state response over a wide range of operating conditions which is suitable for testing an extremum seeking controller chasing an unknown optimum. The state-space description of the model is,

$$\dot{\mathbf{x}} = \mathbf{f}(t, \mathbf{x}, \mathbf{u}), \tag{1a}$$
$$\mathbf{y} = \mathbf{h}(t, \mathbf{x}, \mathbf{u}), \tag{1b}$$

where the state vector is $\mathbf{x} = [x_w,\ x_s,\ x_r,\ x_f]^T$, the input vector is $\mathbf{u} = [u_w,\ u_o,\ u_\phi]^T$ and the output vector is $\mathbf{y} = [J_T,\ P_M,\ Q_s,\ \psi]^T$. The state equations are,

$$\dot{x}_w = u_w - Q_w, \tag{2a}$$
$$\dot{x}_s = (1-\alpha_r)\frac{u_o}{\rho_o} - Q_s + Q_{rc}, \tag{2b}$$
$$\dot{x}_r = \alpha_r \frac{u_o}{\rho_o} - Q_{rc}, \tag{2c}$$
$$\dot{x}_f = \alpha_f \frac{u_o}{\rho_o} - Q_f + Q_{fp}, \tag{2d}$$

where x_w, x_s, x_r and x_f represent the volume of the water, solids, rocks and fines in the grinding mill, α_f is the fraction of fines in u_o and α_r is the fraction of rock in u_o. The grinding mill discharge flow rates are defined as,

$$Q_w = d_q x_w \varphi \left(\frac{x_w}{x_s + x_w}\right), \tag{3a}$$
$$Q_s = d_q x_w \varphi \left(\frac{x_s}{x_s + x_w}\right), \tag{3b}$$
$$Q_f = d_q x_w \varphi \left(\frac{x_f}{x_s + x_w}\right), \tag{3c}$$

where d_q is the discharge rate constant. The grind of the mill is defined as a ratio of the fines to the solids,

$$\psi = \frac{Q_f}{Q_s}. \tag{4}$$

The fraction of the total mill filled with charge is,

$$J_T = \frac{x_w + x_s + x_r + x_b}{V_{mill}}, \tag{5}$$

where x_b is the volume of steels balls in the mill and V_{mill} is the total volume of the mill. The mill power consumption is modelled as a function of J_T and u_ϕ,

$$P_M(J_T,u_\phi) = P_{max}(u_\phi)\left(1-\delta_v\left(\frac{J_T}{J_{T,P_{max}}(u_\phi)}-1\right)^2 - \delta_s\left(\frac{\varphi}{\varphi_N}-1\right)^2\right), \tag{6}$$

where δ_v and δ_s is the power change parameter for the volume of mill filled and for the volume fraction of solids in the slurry, respectively, φ is the rheology factor and φ_N is the normalization factor. $J_{T,P_{max}}(u_\phi)$ is a parameterized function of the fraction of the mill filled at maximum power draw given by,

$$J_{T,P_{max}}(u_\phi) = -7.52u_\phi^2 + 9.06u_\phi - 2.18, \tag{7}$$

and $P_{max}(u_\phi)$ is a parameterized function of the maximum mill power consumption given by,

$$P_{max}(u_\phi) = \left(-2.70u_\phi^2 + 3.92u_\phi - 1.02\right)\times 10^4, \tag{8}$$

and φ is the rheology factor given by the function,

$$\varphi = \begin{cases} \sqrt{1 - \frac{x_s}{x_w}\left(\epsilon_0^{-1} - 1\right)} & , \text{ if } \frac{x_s}{x_w} \le \left(\epsilon_0^{-1} - 1\right)^{-1} \\ 0 & , \text{ if } \frac{x_s}{x_w} > \left(\epsilon_0^{-1} - 1\right)^{-1} \end{cases} \tag{9}$$

where ϵ_0 is the maximum fraction of solids by volume of slurry at zero slurry flow. The ratio x_s/x_w describes the

volume of the solids to water in the slurry. The grinding operation results in the consumption of the grinding media, resulting in the production of fine and solid particles. The ball filling (x_b) is assumed to be kept constant during the grinding operation, which is valid as the trend of grind curves remain parabolic for a varying ball filling and only the peaks of the performance indicators shift (Powell et al., 2009). The rock consumption (Q_{rc}) and fines produced (Q_{fp}) functions, respectively, are defined as,

$$Q_{rc} = \frac{P_M(J_T, u_\phi)}{\rho_o K_{rc}(J_T, u_\phi)}, \tag{10a}$$

$$Q_{fp} = \frac{P_M(J_T, u_\phi)}{\rho_o K_{fp}(J_T, u_\phi)}. \tag{10b}$$

The factors K_{rc} and K_{fp} are functions which indicate the energy required per tonne of rocks consumed and fines produced, respectively,

$$\begin{aligned} K_{rc}(J_T,u_\phi)=\big(&(-0.478u_\phi^3-3.06u_\phi^2+1.55u_\phi-0.183)J_T^3\\ &+(2.68u_\phi^3+5.13u_\phi^2-2.92u_\phi+0.355)J_T^2\\ &+(-3.15u_\phi^3-2.61u_\phi^2+1.78u_\phi-0.226)J_T\\ &+(1.05u_\phi^3+0.361u_\phi^2-0.352u_\phi+0.0472)\big)\times10^6, \end{aligned} \tag{11a}$$

$$\begin{aligned} K_{fp}(J_T,u_\phi)=\big(&(-3.73u_\phi^3+0.602u_\phi^2+0.301u_\phi-0.0487)J_T^3\\ &+(8.76u_\phi^3-1.97u_\phi^2-0.453u_\phi+0.0877)J_T^2\\ &+(-6.82u_\phi^3+1.91u_\phi^2+0.180u_\phi-0.05)J_T\\ &+(1.77u_\phi^3-0.581u_\phi^2-0.007u_\phi+0.009)\big)\times10^6. \end{aligned} \tag{11b}$$

5. EXTREMUM SEEKING CONTROL

Extremum seeking control (ESC) is an optimization technique that maximizes an objective function by exploring through an unknown static map and steering the system towards the optimal operating conditions. It is fundamentally a gradient-search method that is dependent on a measurable, convex objective function and does not rely on the explicit knowledge of the process behaviour. Perturbation-based ESC employs a periodic excitation signal added to the input of the system, which is used to obtain the gradient information of the objective function. The periodic signal enables the controller to continuously track the unknown time-varying optimum subject to disturbances. The controller adapts the input based on the measured change in the system output due to the perturbed input, hence, the adaptation dynamics are based on the average trend of the gradient.

The perturbation-based ESC scheme is shown in Fig. 5 and the closed-loop system dynamics with ESC are described by (Krstić and Wang, 1997),

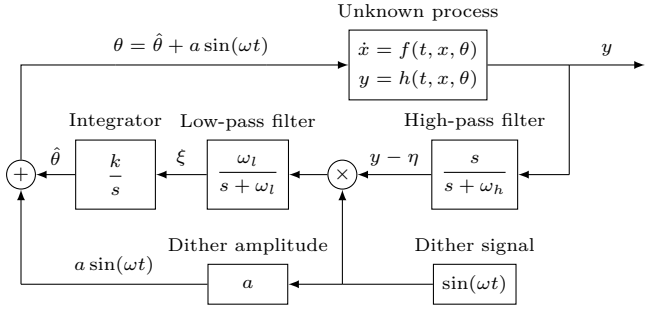

Fig. 5. Perturbation-based extremum seeking scheme (Krstić and Wang, 1997).

$$\dot{x} = f(t, x, \theta), \tag{12a}$$

$$y = h(t, x, \theta), \tag{12b}$$

$$\dot{\hat{\theta}} = k\xi, \tag{12c}$$

$$\dot{\xi} = -\omega_l \xi + \omega_l (y - \eta) a \sin(\omega t), \tag{12d}$$

$$\dot{\eta} = -\omega_h \eta + \omega_h y, \tag{12e}$$

where the unknown process dynamics are described by $\dot{x}$, y is the measurable output, ω_l and ω_h are the cut-off frequencies for the low-pass and high-pass filters, respectively. The state of the high-pass filter is indicated by η, which separates the variation in the measured output from the average value, resulting in the filtered output, $y - \eta$. The signal is demodulated and the low-pass filter extracts the gradient (ξ) of the optimized variable. The sign of the gradient is used to determine the direction of the extremum, which is driven to zero by an integrator with gain, k, and the best estimate of the optimal input ($\hat{\theta}$) converges towards the unknown optimal input. The input (θ) to the process consists of the best estimate of the optimal input ($\hat{\theta}$) and the periodic dither signal,

$$\theta = \hat{\theta} + a\sin(\omega t), \tag{13}$$

where a and ω is the perturbation amplitude and frequency, respectively. Applying extremum seeking to a dynamic process requires a sufficient time-scale separation between the perturbation frequency and the process dynamics to enable the optimizer to search through an unknown static map. Therefore, it is required that a suitable perturbation frequency is chosen such that the process dynamics operate at the fastest time-scale, followed by the medium time-scale dynamics of the perturbation signal, and the optimization occurs at the slowest time-scale. Further, the cut-off frequency of the high-pass and low-pass filter should be lower than the chosen perturbation frequency, and k needs to be chosen to be sufficiently small (Krstić and Wang, 1997).

6. RESULTS

The simulations in this section demonstrate that the ESC can act as a supervisory controller to steer the grinding mill toward optimal operating conditions. The process and ESC initial conditions are provided in Table 3 and the parameters used in the simulations for the model described in Eq. (1)-(10) are summarized in Table 4. A PI-controller is used to regulate the water to solids ratio at $x_w/x_s = 0.9$ to ensure that the discharge slurry from the grinding mill is a flowing mixture and another PI-controller is used to regulate J_T at a specified setpoint. The ESC optimizes the mill performance by manipulating the setpoint of J_T or by directly manipulating u_ϕ. If J_T is used, the ESC perturbations are added to the setpoint of J_T and the PI-controller aims to track the perturbed setpoint, whereas,

Table 3. Initial process and ESC conditions.

	Optimization of Q_s	Optimization of ψ
$\mathbf{u}(0)$	$[61.13,\ 183.4,\ 0.65]^T$	$[94.98,\ 284.95,\ 0.70]^T$
$\mathbf{x}(0)$	$[6.96,\ 7.74,\ 41.7,\ 6.25]^T$	$[10.82,\ 12.02,\ 2.36,\ 6.80]^T$
$\hat{\theta}(0)$	0.35	0.20
$\xi(0)$	0	0
$\eta(0)$	67.93	0.57

Table 4. Parameter values.

Variable	Value	Description
α_f	0.1 (-)	Fraction of fines in u_o
α_r	0.5 (-)	Fraction of rocks in u_o
ρ_o	2.7 (t/m^3)	Ore density
d_q	36.4 (1/h)	Discharge rate constant
x_b	16.4 (m^3)	Volumetric filling of balls in mill
V_{mill}	208 (m^3)	Total mill volume
δ_v	0.923 (-)	Power change parameter for the volume of mill filled
δ_s	0.923 (-)	Power change parameter for volume fraction of solids in the slurry
φ_N	0.509 (-)	Rheology normalization factor
ϵ_0	0.6 (-)	Maximum fraction of solids by volume of slurry at zero slurry flow

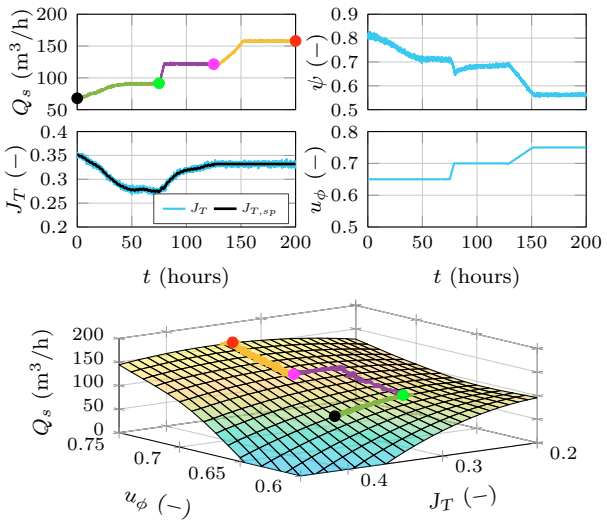

Fig. 6. Throughput (Q_s) optimization. (The black ∘ indicates the initial conditions, u_ϕ is incremented at the green ∘, the magenta ∘ indicates the ESC switch from perturbing J_T to u_ϕ and the red ∘ indicates the final conditions.)

for u_ϕ, the ESC can directly perturb the mill speed. White Gaussian noise with a noise level of -5 dB is added to Q_s, and -50 dB is added to J_T and ψ to evaluate the performance of the ESC subject to measurement noise. Furthermore, the ESC is restricted to explore in a region that is defined by the grind curves, $J_T \in [0.20, 0.45]$ and $u_\phi \in [0.60, 0.75]$.

6.1 Throughput Optimization

The ESC tuning parameters used to optimize Q_s are chosen as $a = 0.001$, $\omega = 2$ rad/h, $k = 25$, $\omega_h = 1.5$ rad/h and $\omega_l = 0.1$ rad/h. In Fig. 6, the ESC is initially set to optimize Q_s by perturbing the setpoint of J_T while maintaining u_ϕ constant. The ESC converges to an average peak of $Q_s = 90.5$ m^3/h. The mill speed is incremented to $u_\phi = 0.70$ at $t = 75$ h over a 4 hour period and the process converges to a new average peak of $Q_s = 121.7$ m^3/h. At $t = 125$ h, the ESC is set to optimize Q_s by perturbing u_ϕ while J_T is regulated at $J_{T,sp} = 0.33$. The mill speed is driven toward the maximum of $u_\phi = 0.75$ and the process converges to an average peak of $Q_s = 157.6$ m^3/h. The optimal peak is $Q_s = 157.7$ m^3/h.

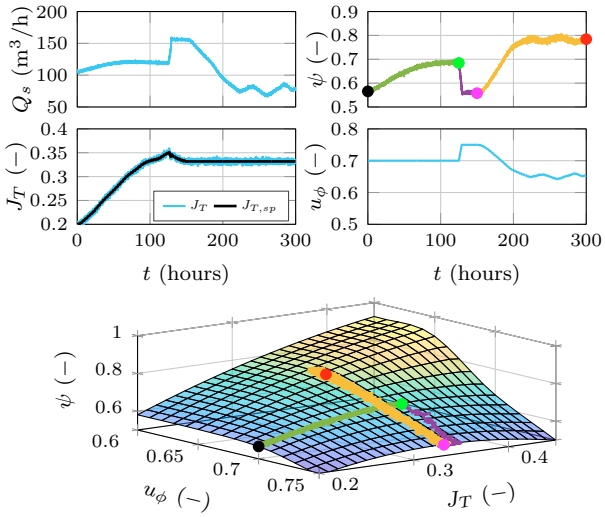

Fig. 7. Grind (ψ) optimization. (The black ∘ indicates the initial conditions, u_ϕ is incremented at the green ∘, the magenta ∘ indicates the ESC switch from perturbing J_T to u_ϕ and the red ∘ indicates the final conditions.)

6.2 Grind Optimization

The ESC tuning parameters used to optimize ψ are chosen as $a = 0.001$, $\omega = 1.8$ rad/h, $k = 4000$, $\omega_h = 1.6$ rad/h and $\omega_l = 0.1$ rad/h. In Fig. 7, the ESC is initially set to optimize ψ by perturbing the setpoint of J_T while maintaining u_ϕ constant. The process converges to an average peak of $\psi = 0.685$, the optimal peak for $u_\phi = 0.70$ is $\psi = 0.69$. The mill speed is incremented from $u_\phi = 0.70$ to $u_\phi = 0.75$ at $t = 125$ h over a 4 hour period and the ESC searches along the grind curve by manipulating the mill load setpoint to locate the new optimal peak for ψ. The ESC converges to a new average peak of $\psi = 0.56$ at $J_T = 0.33$. At $t = 150$ h, the ESC is switched to optimize ψ by perturbing u_ϕ and J_T is regulated at $J_{T,sp} = 0.33$. The ESC converges to an average peak of $\psi = 0.781$ and the optimal peak is $\psi = 0.795$.

The grind curves (Fig. 4) indicate that ψ is maximized at a higher mill load and lower mill speed. In Fig. 7, J_T is seen to be continuously increasing for $t < 125$ h when manipulating the mill load. If the process were to be initially set to operate at a lower mill speed ($u_\phi < 0.65$) a similar trend would be observed if the ESC is used to maximize ψ with J_T. However, the process would converge toward a peak located at a high mill load ($J_T > 0.45$) and result in the mill to overfill, requiring the operation to stop. Therefore, there should be some precaution when choosing the mill speed and using the mill load to optimize ψ. Similarly, precaution should be taken when optimizing Q_s with u_ϕ at lower mill fillings as the optimal peak of Q_s could result in u_ϕ to converge to a high mill speed. Consequently, the position of the toe and shoulder of the mill load shifts, resulting in the grinding media to make direct contact with the mill liners and damaging the equipment (Liddel and Moys, 1988). Therefore, constraints should be imposed to limit the extent to which the ESC can adapt J_T and u_ϕ.

In both optimization cases, the noise level of the measured output (-5 dB $= 0.562$ and -50 dB $= 0.003$) is higher than the perturbation amplitude ($a = 0.001$). This demonstrates the high-pass and low-pass filters are adequately tuned and the ESC can effectively steer the process towards the optimum. However, in Fig. 7, the ESC fails to maintain the process near steady state for $t > 200$ h which can be attributed to the influence of the noise.

Applying ESC to a multi-output process presents a scenario where a single output is optimized and the remaining outputs are uncontrolled. For example, in Fig. 6 the trajectory of ψ is dependent on the operating conditions that optimizes Q_s, which due to inverse relationship between Q_s and ψ, results in the observed decrease in ψ. Ideally, the variation in ψ should be minimized to achieve effective separation of the product in downstream processes. Hence, for a multi-input process, additional degrees of freedom can be utilized to regulate the uncontrolled output at a setpoint, i.e., an inner loop regulatory controller can manipulate u_ϕ to control ψ and the ESC can manipulate the J_T setpoint to optimize Q_s.

7. CONCLUSION

The advantage of ESC is that at all times, the variable being optimized is continuously steered in the direction of the optimum subject to the disturbances and changes in the optimization strategy. However, grinding mills have slow dynamics, therefore, a low perturbation frequency is required for extremum seeking to be effective. The slow convergence rate can be seen in Fig. 7, where the process converged toward the peak after 95 hours from its initial conditions.

A shortcoming of perturbation-based ESC is that the continuous perturbation is observed in the measured output. For example, ψ should remain close to steady-state conditions for improved separation in the downstream processes, but the oscillations around the steady-state optimum could disturb the separation process. Hence, the advantages of employing ESC should ultimately outweigh the potential economic loss as a result of the perturbations. Additionally, the measurement noise can affect the direction of the optimization if the ESC is not adequately tuned. The perturbation amplitude should be chosen large enough to overcome the measured noise levels of the optimized variable, but small enough to obtain an acceptable variation in the optimized output once the ESC has converged. Further, increasing the ESC integrator gain can improve the convergence rate performance but it also increases the ESC sensitivity to noise.

Future work will consider optimization of the grinding mill as a multivariable case using J_T and u_ϕ simultaneously to achieve optimal performance between a weighted objective function of Q_s and ψ. The ESC will also be evaluated for a closed grinding mill circuit.

ACKNOWLEDGEMENTS

This work is based on the research supported by the National Research Foundation of South Africa (IRC grant number 130569).

REFERENCES

Bouffard, S.C. (2015). Benefits of process control systems in mineral processing grinding circuits. *Miner. Eng.*, 79, 139–142.

Edwards, R., Vien, A., and Perry, R. (2002). Strategies for the instrumentation and control of grinding circuits. In *Mineral processing plant design, practice, and control*, 2130–2151. Society for Mining, Metallurgy, and Exploration, Vancouver, Canada.

Hodouin, D. (2011). Methods for automatic control, observation, and optimization in mineral processing plants. *J. Process. Contr.*, 21, 211–225.

Krstić, M. and Wang, H. (1997). Design and stability analysis of extremum seeking feedback for general nonlinear systems. In *Proceedings of the 36th Conference on Decision and Control*, 1743–1748. IEEE, San Diego, USA.

le Roux, J.D. and Craig, I.K. (2019). Plant-wide control framework for a grinding mill circuit. *Ind. Eng. Chem. Res.*, 58, 11585–11600.

le Roux, J.D., Craig, I.K., Hulbert, D.G., and Hinde, A.L. (2013). Analysis and validation of a run-of-mine ore grinding mill circuit model. *Miner. Eng.*, 43-44, 121–134.

le Roux, J.D., Olivier, L.E., Naidoo, M.A., and Craig, I.K. (2016). Throughput and product quality control for a grinding mill circuit using non-linear MPC. *J. Process. Contr.*, 42, 35–50.

le Roux, J.D., Steinboeck, A., Kugi, A., and Craig, I.K. (2020). Steady-state and dynamic simulation of a grinding mill using grind curves. *Miner. Eng.*, 152, 106208.

Liddel, K.S. and Moys, M.H. (1988). The effects of mill speed and filling on the behaviour of the load in a rotary grinding mill. *J. S. Afr. I. Min. Metall.*, 2, 49–58.

Lu, X., Krstić, M., Chai, T., and Fu, J. (2020). Hardware-in-the-loop multiobjective extremum-seeking control of mineral grinding. *IEEE T. Contr. Syst. T.*, 1–11.

Maritz, M.G., le Roux, J.D., and Craig, I.K. (2019). Feed size distribution feedforward control for a grinding mill circuit. *IFAC-PapersOnline*, 52(14), 7–12.

Powell, M.S., Morrell, S., and Latchireddi, S. (2001). Developments in the understanding of South African style SAG mills. *Miner. Eng.*, 14, 1143–1153.

Powell, M.S., van der Westhuizen, A., and Mainza, A. (2009). Applying grindcurves to mill operation and optimisation. *Miner. Eng.*, 22, 625–632.

van der Westhuizen, A.P. and Powell, M.S. (2006). Milling curves as a tool for characterising SAG mill performance. In *Mular, et al., (Ed.), Proceedings of International Autogenous and Semiautogenous Grinding Technology 2006*, 217–232. CIM, Vancouver, B.C., Canada.

Wei, D. and Craig, I.K. (2009). Grinding mill circuits - A survey of control and economic concerns. *Int. J. Miner. Process.*, 90, 56–66.

Zhou, P., Lu, S., Yuan, M., and Chai, T. (2016). Survey on higher-level advanced control for grinding circuits operation. *Powder Technology*, 288, 324–338.